Pharm Res (2012) 29:1468–1484
DOI 10.1007/s11095-011-0622-3

RESEARCH PAPER

# Polymeric Nanoparticles Affect the Intracellular Delivery, Antiretroviral Activity and Cytotoxicity of the Microbicide Drug Candidate Dapivirine

José das Neves • Johan Michiels • Kevin K. Ariën • Guido Vanham • Mansoor Amiji • Maria Fernanda Bahia • Bruno Sarmento

Received: 12 August 2011 / Accepted: 26 October 2011 / Published online: 10 November 2011


## ABSTRACT

***Purpose*** To assess the intracellular delivery, antiretroviral activity and cytotoxicity of poly(ε-caprolactone) (PCL) nanoparticles containing the antiretroviral drug dapivirine.

***Methods*** Dapivirine-loaded nanoparticles with different surface properties were produced using three surface modifiers: poloxamer 338 NF (PEO), sodium lauryl sulfate (SLS) and cetyl trimethylammonium bromide (CTAB). The ability of nanoparticles to promote intracellular drug delivery was assessed in different cell types relevant for vaginal HIV transmission/microbicide development. Also, antiretroviral activity of nanoparticles was determined in different cell models, as well as their cytotoxicity.

***Results*** Dapivirine-loaded nanoparticles were readily taken up by different cells, with particular kinetics depending on the cell type and nanoparticles, resulting in enhanced intracellular drug delivery in phagocytic cells. Different nanoparticles showed similar or improved antiviral activity compared to free drug. There was a correlation between increased antiviral activity and increased intracellular drug delivery, particularly when cell models were submitted to a single initial short-course treatment. PEO-PCL and SLS-PCL nanoparticles consistently showed higher selectivity index values than free drug, contrasting with high cytotoxicity of CTAB-PCL.

***Conclusions*** These results provide evidence on the potential of PCL nanoparticles to affect *in vitro* toxicity and activity of dapivirine, depending on surface engineering. Thus, this formulation approach may be a promising strategy for the development of next generation microbicides.

**KEY WORDS** cell uptake · HIV/AIDS · microbicides · nanotechnology · poly(ε-caprolactone)

## ABBREVIATIONS

| | |
|---|---|
| $CC_{50}$ | 50% cytotoxic concentration |
| CTAB | cetyl trimethylammonium bromide |
| DIC | differential interference contrast |
| DLS | dynamic light scattering |
| DMSO | dimethyl sulfoxide |
| $EC_{50}$ | 50% effective concentration |
| FACS | fluorescence-activated cell sorting |
| FBS | fetal bovine serum |

J. das Neves (✉) • M. F. Bahia • B. Sarmento
Laboratory of Pharmaceutical Technology, LTF/CICF
Faculty of Pharmacy, University of Porto
Rua Aníbal Cunha, 164, 4050-047 Porto, Portugal
e-mail: j.dasneves@gmail.com

J. Michiels • K. K. Ariën • G. Vanham
Virology Unit, Department of Microbiology
Institute of Tropical Medicine
Antwerpen, Belgium

G. Vanham
Department of Biomedical Sciences, Faculty of Pharmacology
Biomedical and Veterinary Sciences, University of Antwerpen
Antwerpen, Belgium

G. Vanham
Faculty of Medicine and Pharmacology, University of Brussels
Brussels, Belgium

M. Amiji
Department of Pharmaceutical Sciences, School of Pharmacy
Northeastern University
Boston, Massachusetts, USA

B. Sarmento
CICS—Centro de Investigação em Ciências da Saúde
Department of Pharmaceutical Sciences
Instituto Superior de Ciências da Saúde-Norte
Gandra, Portugal

| | |
|---|---|
| LDH | lactate dehydrogenase |
| MOI | multiplicity of infection |
| Mo-DC | monocyte-derived dendritic cells |
| Mo/Mac | monocyte/macrophages |
| MTS | 3-(4,5-dimethylthiazol-2-yl)-5-(3-carboxymethoxyphenyl)-2-(4-sulfophenyl)-2H-tetrazolium assay |
| NNRTI | non-nucleoside reverse transcriptase inhibitor |
| PBL | peripheral blood lymphocytes |
| PBMCs | peripheral blood mononuclear cells |
| PBS | phosphate buffered saline |
| PCL | poly(ε-caprolactone) |
| PdI | polydispersity index |
| PEO | poly(ethylene oxide) |
| PHA | phytohemagglutinin |
| PPO | poly(propylene oxide) |
| SEM | scanning electron microscopy |
| SLS | sodium lauryl sulfate |
| SVF | simulated vaginal fluid |
| WST-1 | water soluble tetrazolium-1 assay |

## INTRODUCTION

Prevention is a keystone strategy in the fight against HIV/AIDS. Safe sexual practices, particularly consistent condom use, have been shown to be a difficult objective to accomplish, while the development of effective vaccines has failed so far (1). Alternative strategies such as oral antiretroviral pre-exposure prophylaxis and microbicides have been proposed and different studies have been performed or are still ongoing (2,3). In particular, proof of concept for vaginal microbicides has been recently achieved in the CAPRISA 004 study (4). After several initial failures using products based on non-specific antiviral compounds (3), this Phase IIb clinical trial found partial but significant protection against HIV acquisition upon the vaginal application around the time of sexual intercourse of a gel containing the nucleotide reverse transcriptase inhibitor tenofovir (4). Current studies are now focusing on getting further confirmatory data for tenofovir gel and other promising products containing antiretroviral drugs with specific and potent activity against HIV-1, namely the non-nucleoside reverse transcriptase inhibitor (NNRTI) dapivirine (5).

In order to exert antiretroviral activity and protect from infection, RTIs need to achieve sufficient and steady intracellular levels in HIV target cells, particularly those implicated in the initial steps of infection, such as $CD4^+$ T cells, intra-epithelial dendritic (Langerhans) cells and macrophages (6–8). In addition, prolonged local tissue concentration seems to be correlated with effective protection (9). Up to now, most strategies for vaginal administration of microbicide drugs relied on conventional dosage forms, mostly hydrophilic gels, but advanced microbicide formulation is expected to play an important role in obtaining enhanced efficacy and safety (10). In particular, nanotechnology-based microbicides have been proposed (11–13) and have been shown to provide a durable drug barrier within the cervicovaginal epithelial lining, allowing sustained drug release and increasing intracellular drug delivery (14,15). However, the kinetics and enhancement in intracellular drug concentrations provided by nanoencapsulation and its contribution to the protection against HIV infection is not yet fully understood. Previous reports by Amiji and collaborators showed that poly(ethylene oxide)-modified poly(ε-caprolactone) (PEO-PCL) nanoparticles provide a good platform for achieving enhanced intracellular concentrations of encapsulated drugs in various cell lines by means of non-specific endocytosis (16–18). In this paper we report on the development of differently engineered poly(ε-caprolactone) (PCL) nanoparticulate systems containing the NNRTI candidate microbicide drug dapivirine and their ability to promote increased intracellular levels in different cell types relevant to microbicide development. Additionally, we evaluated the cytotoxicity of drug-loaded nanoparticles to various female genital and anorectal epithelial cell lines, and their ability to inhibit HIV infection in different *in vitro* models.

## MATERIALS AND METHODS

### Materials

Dapivirine was a kind offer from the International Partnership for Microbicides (Silver Spring, MD, USA). PCL with molecular weight of 14,800 Da was purchased from Polysciences Inc. (Warrington, PA, USA). Poloxamer 338 NF (Pluronic® F 108 NF), a triblock copolymer of poly (ethylene oxide) (PEO) and poly(propylene oxide) (PPO) (PEO-PPO-PEO), was acquired from BASF (Mount Olive, NJ, USA), sodium lauryl sulfate (SLS) from Fisher Scientific (Fair Lawn, NJ, USA), cetyl trimethylammonium bromide (CTAB) from Spectrum Chemical Mfg. Corp. (Gardena, CA, USA), and rhodamine-123 from Invitrogen (Carlsbad, CA, USA). All other chemicals and reagents were of analytical grade or equivalent.

### Preparation of Nanoparticles

Dapivirine-loaded PCL nanoparticles were obtained by a solvent displacement method modified from Amiji *et al.* (16,17). Briefly, 34 mg of PCL, 6 mg of surface modifier (PEO-PPO-PEO, SLS or CTAB) and 6 mg of dapivirine were dissolved in 2 mL of acetone/ethanol (1:1) with the help of mild heating (37°C). The mixture was then added

dropwise to 20 mL of deionized water under magnetic stirring, which was continued overnight. Obtained nanoparticles were recovered by ultracentrifugation at 90,140×*g* for 30 min and the resulting pellet was washed twice with 20 mL of deionized water. The same procedure was used to obtain blank nanoparticles, i.e. without the incorporation of dapivirine, and fluorescent nanoparticles by substituting dapivirine with rhodamine-123 (0.5% *w/w* loading). Freeze-drying of nanoparticles was performed if required.

## Characterization of Nanoparticles

Mean particle diameter and polydispersity index (PdI) were determined by dynamic light scattering (DLS) at 90.0° scattering angle and 20°C using a ZetaSizer Nano ZS (Malvern Instruments Ltd., Worcestershire, UK). Zeta potential was also assessed with the same equipment by combination of laser Doppler anemometry (LDA) and phase analysis light scattering (PALS). Association efficiency and drug loading were determined indirectly by dosing the amount of non-encapsulated drug from supernatants resulting from nanoparticle washing and separation. Dapivirine was assayed by a validated HPLC-UV method previously developed (19).

Drug release from nanoparticles was determined in a simulated vaginal fluid (SVF, pH 4.2) adapted from a previously described recipe (20), or in phosphate buffered saline (PBS, pH 7.4). Due to the very poor water solubility of dapivirine (logP=6.3 (21)), polysorbate 80 at a concentration of 2% (*w/v*) was added to both media in order to maintain sink conditions throughout the experiment (volume of the dissolution medium was at least three times higher than the volume required to achieve a saturated solution of dapivirine). Freeze-dried nanoparticles were transferred to screw capped cylindrical glass flasks containing 20 mL of media and placed in a horizontal shaking water bath (150 strokes/min) at 37.0±0.1°C. At different time points, the flasks content was centrifuged and a sample of the supernatant was removed and filtered by a 0.2 μm filter for drug assay by HPLC-UV and replaced with fresh media. Experiments were performed in triplicate.

Scanning electron microscopy (SEM) images of nanoparticles were obtained using a Hitachi S-4800 FE-SEM (Hitachi High Technologies America, Inc., Pleasanton, CA, USA) at an acceleration voltage of 3.0 kV, after sputter-coating of freeze-dried nanoparticles with a gold-palladium alloy.

## Cell Lines, Primary Cell Isolation, and Culture Conditions

Various immortalized cell lines and primary cells with relevance for vaginal/rectal drug delivery and microbicide development were used. VK2/E6E7 human vaginal epithelial cells (ATCC, Manassas, VA, USA) were cultured in keratinocyte serum-free medium (K-SFM) (Invitrogen) supplemented with 50 mg/mL bovine pituitary extract, 0.1 ng/mL recombinant human epidermal growth factor, 100 U/mL penicillin, 100 mg/mL streptomycin, and calcium chloride (final concentration of 0.4 mM), and used at passages 49–62. HeLa human cervical cells, Caco-2 human colorectal epithelial cells, and J774A.1 mice monocyte/macrophages (Mo/Mac), all from ATCC, were cultured in DMEM with GlutaMAX™-I (Invitrogen) supplemented with 10% fetal bovine serum (FBS; Invitrogen), 100 U/mL penicillin and 100 μg/mL streptomycin (Invitrogen), and 0.25 μg/mL amphotericin B (Invitrogen), and used at passages 40–42, 66–80, and 6–10, respectively. HEC-1-A human endometrial cells (ATCC) were maintained in McCoy's 5A modified medium (Invitrogen), 10% FBS (Invitrogen), 100 U/mL penicillin and 100 μg/mL streptomycin (Invitrogen), and 0.25 μg/mL amphotericin B (Invitrogen), and used at passages 4–6. TZM-bl cells (NIBSC, Hertfordshire, UK) were maintained in DMEM (Lonza Sprl, Verviers, Belgium) supplemented with 50 μg/mL of gentamicin sulfate (Lonza), L-glutamine (final concentration of 6 mM) (Lonza), and 10% FBS (Sigma-Aldrich, Inc., St. Louis, MO, USA) (further referred to as TZM-bl medium), and used at passages 24–38.

Commercially available DC-100 dendritic (Langerhans) cells (MatTek Corp., Ashland, MA, USA), generated from $CD34^+$ progenitor cells harvested from human umbilical cord blood (22), were maintained in Dendritic Cell Maintenance Medium (DC-MM; MatTek Corp.) consisting of RPMI-1640 containing a proprietary mixture of cytokines. Cells were used within 14 days following reception. Peripheral blood mononuclear cells (PBMCs) were isolated by density gradient centrifugation from buffy coats of healthy adult donors obtained from the Blood Transfusion Center of the Red Cross, Antwerpen, Belgium, using Lymphoprep™ (Axis-Shield PoC AS, Oslo, Norway). PBMCs were stimulated for 2–3 days in RPMI-1640 (Lonza) added with 50 μg/mL gentamicin sulfate (Lonza), and L-glutamine at a final concentration of 4 mM (Lonza) (further referred to as basic medium), and further supplemented with 0.5 μg/mL phytohemagglutinin (PHA; Oxoid Limited, Basingstoke, UK), 2 μg/mL hexadimethrine bromide (Sigma-Aldrich), and 15% FBS (Sigma-Aldrich). Subsequently, PBMCs were cultured for 1–2 days in basic medium supplemented with 200 UI/mL of recombinant human IL-2 (Gentaur, Brussels, Belgium), 5 μg/mL hydrocortisone (VWR International Ltd., Poole, England), 2 μg/mL hexadimethrine bromide (Sigma-Aldrich), and 15% FBS (Sigma-Aldrich), further referred to as IL-2 medium. Monocyte-derived dendritic cells (Mo-DC) and $CD4^+$ T cells (T4 cells) were generated from buffy coats of healthy adult donors by modifying a previously developed method (23–25). Briefly, PBMCs were isolated by double

density gradient centrifugation in Lymphoprep™. PBMCs were then separated into peripheral blood lymphocytes (PBL) and monocytes with magnetic CD14 beads (MACS® CD14 MicroBeads, Miltenyi Biotec, Bergisch Gladbach, Germany) using a separation column (MACS® 25 LS separation column, Miltenyi Biotec) in the presence of a magnetic field (MACS® magnetic cell separator, Miltenyi Biotec). The CD14 negative fraction, corresponding to PBL, was frozen and kept in liquid nitrogen until further processing. The CD14+ fraction (i.e. monocytes) was differentiated into Mo-DC by 7-day culture in basic medium supplemented with 10% FBS (Sigma-Aldrich), 20 ng/mL IL-4 (Invitrogen) and granulocyte-macrophage colony-stimulating factor (GM-CSF; Gentaur) (26). On the experiment day, T4 cells were isolated from PBL using a $CD4^+$ isolation kit (Dynal® CD4 positive isolation kit, Invitrogen) as previously described (24). Phenotypic characterization of Mo-DC and T4 cells was performed by FACS using fluorescently labeled antibodies for specific surface markers of these cells.

## Nanoparticles Uptake and Intracellular/Cell Associated Drug Levels

Qualitative cellular uptake of nanoparticles in VK2/E6E7 cells, HeLa cells, TZM-bl cells, Mo/Mac, PBMCs, and DC-100 cells was assessed by fluorescence microscopy. Briefly, fluorescent nanoparticles were dispersed in culture medium at a concentration of 0.01% (*w*/*v*) and incubated with cells (37°C/5% $CO_2$). At different time points ranging from 15 min to 4 h, cells were washed twice with PBS (pH 7.4) and stained for DNA with Hoechst 33342 dye (Invitrogen). Intracellular uptake was assessed using an Olympus IX51 inverted microscope equipped with an Olympus U-RFL-T fluorescence mercury lamp (Olympus America Inc., Center Valley, PA, USA), or a Nikon Eclipse E400 equipped with a Nikon HB-10104AF fluorescence mercury lamp (Nikon Instruments Inc., Melville, NY, USA). Obtained images were processed with ImageJ software. All treatments were performed at least in triplicate. Cell viability during the experiments was assessed by performing a trypan blue exclusion test (27).

Intracellular/cell associated drug levels were assessed by dosing the amount of dapivirine associated with VK2/E6E7 cells ($2\times10^5$ cells), HeLa cells ($2\times10^5$ cells), TZM-bl cells ($2\times10^5$ cells), Mo/Mac ($2\times10^5$ cells), PBMCs ($3.75\times10^5$ cells), and DC-100 cells ($0.5\times10^5$ cells) after incubation with nanoparticles/free dapivirine dispersed in culture medium at different time points and concentrations. In all cases, a small amount of dimethyl sulfoxide (DMSO) was used to disperse the free drug in culture media (final DMSO concentration was ≤0.05% *v*/*v* in all cases). Under similar conditions, dapivirine is known to originate aggregates smaller than 200 nm in diameter (21); in our case, we determined the mean value to be 69±28 nm by DLS. The range of concentrations tested was chosen considering the antiviral and cytotoxic concentrations previously reported for dapivirine (28,29). After incubation (37°C/5% $CO_2$), cells were washed at least twice with PBS (pH 7.4) and disrupted with a lysis buffer (10 mM Tris–HCl pH 7.4, 2 mM EDTA pH 8.0, 150 mM NaCl, 0.876% (*w*/*v*) Brij® 97, 0.125% (*w*/*v*) Tween® 20, and one tablet/50 mL of protease inhibitor cocktail (cOmplete, Mini, EDTA-free; Roche Diagnostics, Indianapolis, IN, USA)). Obtained suspensions were centrifuged (13,000 rpm, 10 min) and supernatant was collected and assayed for soluble protein content with a colorimetric-based commercial kit (Pierce® BCA Protein Assay Kit, Thermo Scientific, Rockford, IL, USA). Precipitation of protein content was then induced by the addition of acetonitrile to the remaining supernatant (2:1) and separated by centrifugation (13,000 rpm, 10 min). Dapivirine was determined from the obtained supernatant by a validated bioanalytical HPLC-UV method: Dionex UltiMate 3000 system; Waters Xterra® RP18, 5 µm, 4.6×150 mm column with a Merck LiChrospher® 100 RP-18, 5 µm guard column; temperature 20°C; mobile phase consisting of acetonitrile:0.1% TFA solution in gradient mode, changing from an initial ratio of 35:65 to 73:27 over 6.5 min, remaining constant up to 9.0 min, and then returning to 35:65 over 1 min (12 min total run time); 1.0 mL/min flow rate; diphenylamine as an internal standard; detection at 290 nm for dapivirine and internal standard; 50 µL injection volume; lower limit of quantification was 0.02 µg/mL (das Neves *et al.*, manuscript in preparation). All conditions were performed in triplicate in three different experiments. Cell viability at the maximum time of incubation (6 h) and maximum concentration (10 µM) used was assessed using a commercially available kit based on the bioreduction of 3-(4,5-dimethylthiazol-2-yl)-5-(3-carboxymethoxyphenyl)-2-(4-sulfophenyl)-2H-tetrazolium (MTS) by metabolically active cells (CellTiter 96® AQueous One Solution Cell Proliferation Assay, Promega, Madison, WI, USA), further referred to as MTS assay. This kit was preferred to the previously used trypan blue exclusion test, which test cell membrane integrity, in order to minimize possible inaccuracies associated with this last (30).

## Virus

The HIV-1 subtype B strain Ba-L (CCR5-tropic) (NIH AIDS Research & Reference Reagent Program, Rockville, MD, USA) was used in all experiments. This strain was selected as a model to be used in all experiments since sexual HIV transmission is mostly associated with R5 viruses (8). Stocks of cell-free virus were prepared by replicating HIV-1 Ba-L in PHA/IL-2 stimulated PBMCs from HIV negative donors (23).

### Inhibition of Cell Infection by HIV

Three different assays were used to evaluate the antiviral activity of nanoparticles and free dapivirine: (i) Tat-regulated LTR-driven luciferase reporter gene assay in TZM-bl cells (31,32), (ii) inhibition of viral p24 production in PHA/IL-2 stimulated PBMCs (33), and (iii) inhibition of viral p24 production in a Mo-DC/T4 cells co-culture model (25,28).

The TZM-bl cell line is derived from HeLa cells by genetically engineering in order to express CD4 and CCR5, and to contain Tat-inducible luciferase and β-galactosidase reporter genes. The expression of the luciferase reporter gene and the presence of D-luciferin (luciferase substrate) confer natural luminescence to these cells. The TZM-bl assay is based on the expression of the luciferase reporter gene after HIV infection due to the presence of its promoter (viral Tat protein), resulting in increased luminescence upon the addition of an adequate luciferase substrate (31,32). Briefly, 10,000 cells were pre-incubated with nanoparticle or free dapivirine dilutions in TZM-bl medium for 2 h. Subsequently, 200 $TCID_{50}$ of Ba-L virus was added and incubated for 48 h (37°C/7% $CO_2$) in the presence of an infectivity enhancer, DEAE-dextran (15 μg/mL; Sigma-Aldrich). Luciferase activity was then determined by adding a luciferase substrate (steadylite plus®, PerkinElmer Inc., Waltham, MA, USA) and the resulting luminescence, expressed as relative luminescence units, measured with a luminometer (model TriStar LB941, Berthold Technologies N.V./S.A., Vilvoorde, Belgium). Results were represented as percentage values of the positive control (medium only). Three-fold replicates were performed in three different independent experiments.

Inhibition of infection in stimulated PBMCs was performed by modifying a previously reported method (33). Briefly, 75,000 cells were pre-incubated with dilutions of nanoparticles or free drug in IL-2 medium for 2 h. Then, virus was added at a multiplicity of infection (MOI) of $10^{-3}$ for 2 h in the presence of nanoparticles or free drug. After discarding supernatants and washing cells twice with basic medium, two different settings were tested. Either PBMCs were cultured in plain IL-2 medium (single treatment) or treated with nanoparticles/free drug in IL-2 medium (continuous treatment) for 14 days. Half of the culture medium (containing nanoparticles or not) was refreshed twice weekly. Viral growth was assessed at day 14 by harvesting supernatants and analyzing for HIV p24 by a previously developed ELISA assay (28,34). Results were expressed in percentage of positive controls (medium only). Six-fold replicates were performed in each of three independent experiments.

Inhibition of infection in a Mo-DC/T4 cell co-culture model was performed as previously reported (25,28). Briefly, 20,000 Mo-DCs were pre-incubated with nanoparticles or free drug in basic medium supplemented with 10% FBS for 2 h, after which $10^{-3}$ MOI of virus was added for 2 h in the presence of nanoparticles or free drug. Subsequently, Mo-DCs were washed and 100,000 T4 cells added. Co-culture was maintained for 14 days in the presence of nanoparticles (continuous treatment) or in plain basic medium containing 10% FBS (single treatment). Half of the culture medium (containing nanoparticles or not) was refreshed twice weekly. Viral growth was assessed at day 14 by ELISA in the same way as for the PBMC assay. Six-fold replicates were performed in each of three independent experiments.

In each of the three described settings, 50% effective concentration ($EC_{50}$) values were determined from the viral growth percentage *vs.* dapivirine concentration plots by log-logistic regression.

### Evaluation of Nanoparticle Cytotoxicity

Nanoparticle toxicity was assessed by determining the 50% cytotoxic concentration ($CC_{50}$) in three female genital epithelial cell lines, namely VK2/E6E7 cells, HeLa cells and HEC-1-A cells, and in the anorectal cell line Caco-2, after 24 h incubation using the MTS assay (Promega) and a commercially available lactate dehydrogenase (LDH) colorimetric cytotoxicity assay kit (LDH Cytotoxicity Detection Kit, Takara Bio Inc., Shiga, Japan). Briefly, cell lines were seeded in 96-well plates (5,000 cells for MTS and 10,000 cells for LDH) and cultured for 24 h. Serial dilutions of nanoparticles or dapivirine were prepared in appropriate medium and added to the cells. Media without FBS were used in the case of LDH. After incubation (37°C/5% $CO_2$), cells were washed twice with PBS (pH 7.4) and the kits were used according to the instructions of the manufacturers. Absorbance was measured using a PowerWave X microplate reader (BioTek Instruments, Inc., Winooski, VT, USA) at 490 nm in both assays. Each concentration was tested in triplicate in three independent experiments.

Additionally, $CC_{50}$ values for nanoparticles and dapivirine were assessed at 2 days incubation for the TZM-bl setting, and after 7 days incubation for the PBMCs and Mo-DC/T4 settings by using the Water Soluble Tetrazolium-1 (WST-1) colorimetric assay (Cell proliferation reagent WST-1, Roche Diagnostics, Mannheim, Germany) according to the manufacturer's instructions. Obtained $CC_{50}$ values were used for calculating the selectivity index (ratio between the mean $CC_{50}$ and the mean $EC_{50}$) of each nanoparticle formulation and free drug, providing an indicator of toxicity. Each concentration was tested in triplicate in three independent experiments.

In all cases, $CC_{50}$ values were calculated by log-logistic regression from cell viability percentage (or cytotoxicity) *vs.* dapivirine concentration plots.

### Statistical Analysis

Statistical analysis of the results was performed with SPSS 17.0 (SPSS Inc., Chicago, IL, USA). One-way ANOVA was used to investigate the differences between formulations at each drug concentration or time point. Post hoc comparisons of the means for each nanoparticle formulation and free dapivirine were performed according to Tukey's HSD test. In all cases, $p<0.05$ was accepted as denoting significance. Log-logistic regression for calculating $EC_{50}$ and $CC_{50}$ values was performed using JMP® software (v. 8.0.2.2, SAS Institute Inc., Cary, NC, USA).

## RESULTS

### Characterization of Nanoparticles

Table I presents the main properties of produced nanoparticles. In common, drug-loaded nanoparticles showed sizes between approximately 180–200 nm, with PdI analysis indicating a homogeneous size distribution. Zeta potential results were in agreement with the type of surface modifier used. Similar properties were obtained for nanoparticles containing no drug or containing rhodamine-123 (Table I). Dapivirine incorporation was around 97%, yielding nearly 13% of the total weight of nanoparticles. The association efficiency was also confirmed by dissolving a known amount of nanoparticles in acetonitrile and dosing the recovered drug. SEM images depicted in Fig. 1 corroborate DLS results in terms of mean size and homogenous distribution, showing round-shaped nanoparticles with smooth surface for all formulations, in accordance with what was previously reported by Amiji and collaborators (16,17). Further, images show no evidence of free drug (amorphous or crystalline) thus supporting the contention that dapivirine is incorporated into the PCL matrix. Figure 2 presents the *in vitro* release profile of dapivirine, showing that the drug is able to be released rapidly from nanoparticles at both pH 4.2 (i.e. healthy vaginal pH) and 7.4. Approximately 75% of the total nanoparticle drug content was released within 2 h at both pH values. However, at pH 7.4 there was a trend for PEO-PCL nanoparticles to release the drug slower, while the opposite occurred for SLS-PCL and CTAB-PCL formulations.

### Evidence of Nanoparticles Uptake and Intracellular Concentrations of Dapivirine

Fluorescent and differential interference contrast (DIC) microscopy images of cells after 1 h of incubation with fluorescent nanoparticles are presented in Fig. 3. Preliminary experiments showed that no significant rhodamine-123 leakage from fluorescent nanoparticles occurred in cell culture media at 37°C for at least 6 h, thus ensuring co-localization of nanoparticles and fluorescence signals. All formulations were readily taken up by all tested cell lines and primary cells, with particular localization of nanoparticles in the cytoplasm as revealed by the brighter fluorescent signal around the nucleus. As a general trend, SLS-PCL nanoparticles presented moderately more intense fluorescence signal at all tested time points and in all cell types, suggesting possible higher internalization for this formulation. Onset of cell uptake of rhodamine 123-loaded nanoparticles was very fast as revealed by the observed fluorescence signal for most of the formulations/cell types after as little as 15 min of incubation (data not shown). The intensity of the fluorescence signal peaked around 1–2 h and remained constant up to 4 h. Cell viability during qualitative cell uptake studies was higher than 90% in all cases as assessed by the trypan blue viability staining.

**Table I** Particle Size, Polydispersity Index (PdI), Zeta Potential, Association Efficiency and Drug Loading of PCL Nanoparticles (Values Expressed as Mean ± Standard Deviation; $n=6$ for Dapivirine-Loaded Nanoparticles; $n=3$ for Drug-Free and Rhodamine-123-Loaded Nanoparticles)

| Surface modifier | Loading | Size (nm) | Polydispersity index (PdI) | Zeta potential (mV) | Dapivirine association efficiency | Dapivirine loading |
|---|---|---|---|---|---|---|
| PEO | – | 204 ± 6 | 0.071 ± 0.024 | −28.7 ± 2.2 | N.A. | N.A. |
| | Dapivirine | 198 ± 7 | 0.120 ± 0.030 | −29.7 ± 5.7 | 97.3% ± 1.3% | 12.7% ± 0.2% |
| | Rhodamine-123 | 196 ± 2 | 0.133 ± 0.042 | −29.2 ± 0.8 | N.A. | N.A. |
| SLS | – | 185 ± 8 | 0.097 ± 0.038 | −57.9 ± 0.6 | N.A. | N.A. |
| | Dapivirine | 182 ± 6 | 0.113 ± 0.028 | −53.1 ± 2.2 | 97.6% ± 0.4% | 12.7% ± 0.1% |
| | Rhodamine-123 | 184 ± 3 | 0.093 ± 0.024 | −53.4 ± 0.7 | N.A. | N.A. |
| CTAB | – | 185 ± 3 | 0.094 ± 0.048 | + 48.1 ± 0.3 | N.A. | N.A. |
| | Dapivirine | 193 ± 8 | 0.170 ± 0.044 | +45.0 ± 3.2 | 97.9% ± 0.3% | 12.8% ± 0.1% |
| | Rhodamine-123 | 188 ± 2 | 0.113 ± 0.036 | +47.8 ± 2.0 | N.A. | N.A. |

*N.A.* not applicable

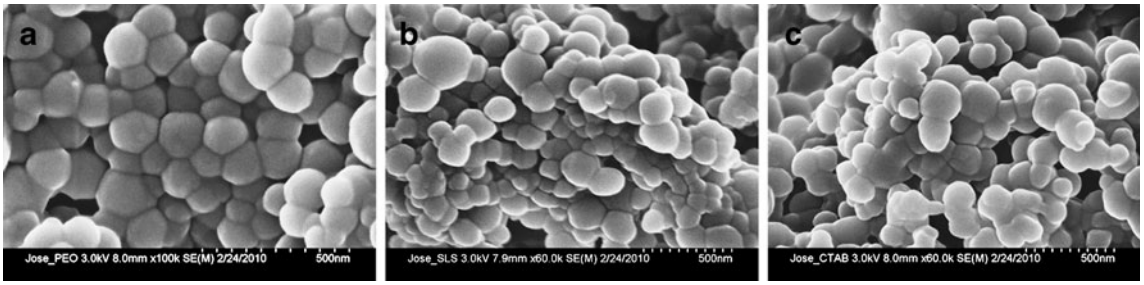


**Fig. 1** SEM images of freeze-dried dapivirine-loaded PEO-PCL (**a**), SLS-PCL (**b**), and CTAB-PCL (**c**) nanoparticles.

Next, we quantified the amount of dapivirine taken up by different epithelial (Fig. 4) and immune cells (Fig. 5) when delivered by the three types of nanoparticles and compared those to the drug levels obtained when free dapivirine was used. Studies were conducted as a function of the initial drug concentration and time of incubation. In all cases, no significant toxicity was observed at the concentration range and maximum time of incubation considered, as assessed by the MTS assay (data not shown). Figure 4A–B shows the results for concentration- and time-dependent uptake in VK2/E6E7 vaginal epithelial cells. CTAB-PCL nanoparticles allowed achieving significantly higher ($p<0.05$) intracellular concentrations of dapivirine at initial incubation concentration from 1 μM (7.2-fold higher levels than for the free drug) to 10 μM (9.6-fold higher levels). Also, increased intracellular levels were observed at all time points from 15 min (around 25-fold higher levels than for free drug) to 6 h (3.2-fold higher levels), with a steady-state being achieved from 2 h onwards. In the case of PEO-PCL and SLS-PCL nanoparticles there were no significant differences when compared with dapivirine both in concentration- and time-dependent experiments, except when testing at 10 μM initial concentrations. Clearly, CTAB-PCL nanoparticles were able to provide higher levels of dapivirine than the other formulations, both in concentration- (except at 0.1 μM) and time-dependent experiments.

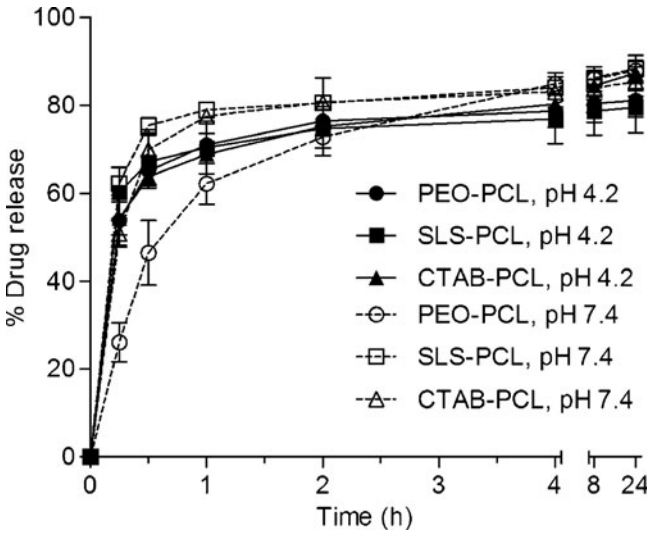


**Fig. 2** *In vitro* drug release profiles of dapivirine from PEO-PCL, SLS-PCL and CTAB-PCL nanoparticles in simulated vaginal fluid (pH 4.2) or phosphate buffered saline (pH 7.4), added of 2% (*w/w*) polysorbate 80 in order to assure sink conditions. Each point represents the mean value and bars the standard deviation ($n=3$). Note the segmented X-axis.

Concentration- and time-dependent uptake for HeLa cervical cells is presented in Fig. 4C–D. All nanoparticle formulations performed better than the free drug in achieving higher concentrations of dapivirine for all concentrations tested ($p<0.05$), except for SLS-PCL at the 0.1 μM condition. However, increases in intracellular drug levels were mild, ranging from 1.5- (PEO-PCL at 2.5 μM) to 3.1-fold (CTAB-PCL at 1 μM). As for time-dependent experiments, significantly higher drug levels were observed up to 2 h for PEO-PCL and SLS-PCL (ranging from 1.7- to 2.5-fold), and up to 6 h in the case of CTAB-PCL nanoparticles (ranging from 2.3- to 4.4-fold). Drug levels increased up to 2 h for PEO-PCL and SLS-PCL, and up to 4 h for CTAB-PCL. From these points on, intracellular drug levels decreased. There were also significant differences between CTAB-PCL nanoparticles and the other formulations after 1 h incubation.

In the case of TZM-bl cells (Fig. 4E–F), drug levels at the concentration-dependent experiments were, in general, moderately higher for the free drug than for the nanoparticle formulations (levels ranging from 0.4- to 1.0-fold as compared to the free drug; higher levels only for SLS-PCL at 0.1 μM), with significant differences being observed ($p<0.05$). These differences were negligible for CTAB-PCL nanoparticles. As for time-dependent experiments, the free drug was able to provide enhanced dapivirine levels in comparison to all nanoparticle formulations up to 2 h. However, these were leveled up around 2 h and even significantly surpassed for all nanoparticles at 6 h. Also, steady intracellular drug levels were achieved fairly rapidly when the free drug was tested, while rising levels were observed for nanoparticle formulations up to 6 h.

Concentration- and time dependent uptake for J774A.1 Mo/Mac is presented in Fig. 5A–B. All PCL nanoparticle formulations performed better in achieving higher dapivirine concentration in this cell line for nearly all initial drug

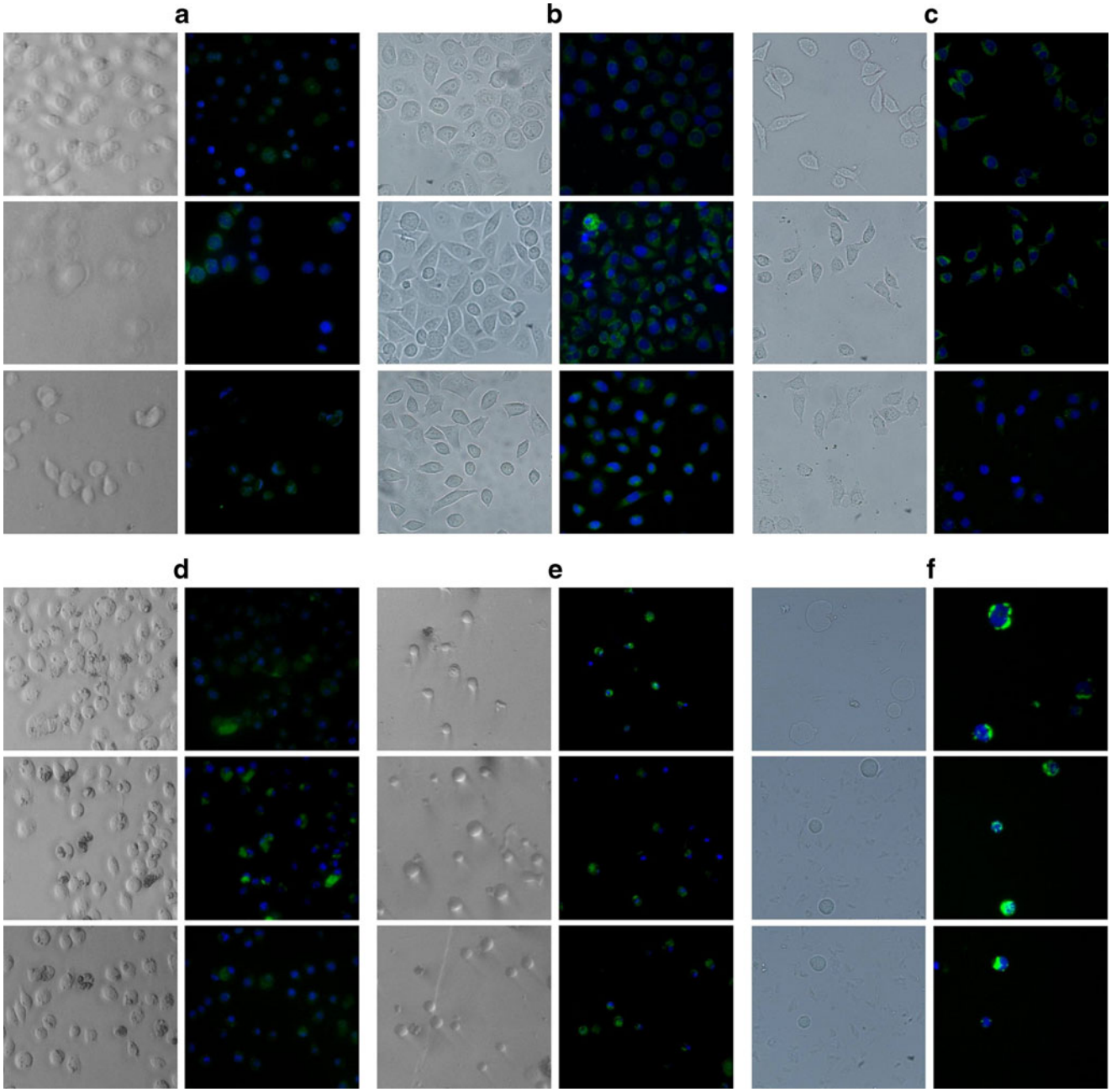


**Fig. 3** Microscopy images of VK2/E6E7 vaginal epithelial cells (**a**), HeLa cervical cells (**b**), TZM-bl cells (**c**), J774A.1 mice monocyte/macrophages (**d**), DC-100 dendritic cells (**e**), and PBMCs (**f**). Images were acquired after 1 h incubation with rhodamine 123-labeled PEO-PCL (*top row*), SLS-PCL (*middle row*), and CTAB-PCL (*bottom row*) nanoparticles. Differential interference contrast (DIC) images (*left column*) and respective fluorescence images (*right column*) were acquired at 40×, except for PBMCs (60×). Green and blue signals on fluorescence images are from rhodamine-123 and Hoechst33342 (DNA labeling), respectively.

concentrations (e.g. around 2.5- to 3.8-fold at 2.5 μM) and time points (e.g. around 11-fold for PEO-PCL and CTAB-PCL nanoparticles, and 5.4-fold for SLS-PCL nanoparticles at 4 h of incubation). In concentration-dependent experiments, there were significant differences ($p<0.05$) among different nanoparticle types, with PEO-PCL formulation scoring better than CTAB-PCL and SLS-PCL nanoparticles, even if significant differences were mostly observed for higher dapivirine concentrations. Results also showed a trend for better uptake with CTAB-PCL nanoparticles when compared to the SLS-PCL formulation but statistical analysis revealed no significant differences. When considering different incubation times, intracellular profile of CTAB-PCL nanoparticles revealed a trend similar to the PEO-PCL formulation, with consistently higher levels than for SLS-PCL nanoparticles. Additionally, the PEO-PCL

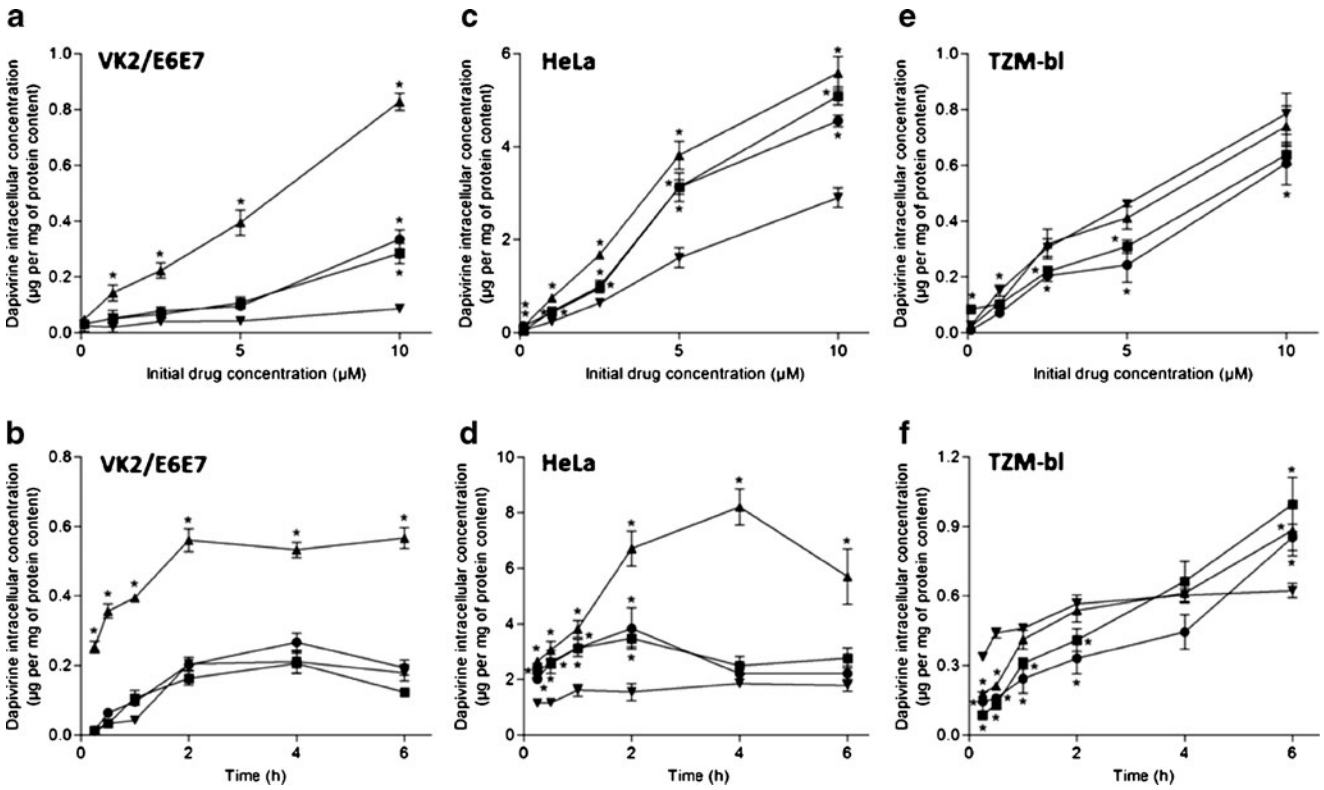


**Fig. 4** Intracellular concentration of dapivirine in VK2/E6E7 vaginal epithelial cells (**a**, **b**), HeLa cervical cells (**c**, **d**), TZM-bl cells (**e**, **f**) as a function of initial drug concentration (**a**, **c**, **e**) and time of incubation (**b**, **d**, **f**). Incubation time was 1 h for dose-dependent studies and drug concentration was held constant at 5 $\mu$M for time-dependent studies. Concentrations are expressed as dapivirine content. Each point represents the mean value and bars the standard deviation of three independent experiments (three replicates per experiment). (*) denotes a significant difference ($p < 0.05$) when compared with the free drug. Legend: dapivirine-loaded PEO-PCL nanoparticles (●), dapivirine-loaded SLS-PCL nanoparticles (■), dapivirine-loaded CTAB-PCL nanoparticles (▲), and free dapivirine (▼).

formulation showed continuous decreasing intracellular dapivirine levels after achieving a maximum at 2 h (13.4-fold higher levels than for the free drug). The same trend was also apparent for the other nanoparticle formulations even if no significant differences were observed for levels in the range of 2–6 h.

Figure 5C–D presents the concentration- and time-dependent uptake for PBMCs. In the case of concentration-dependent uptake, all nanoparticle formulations allowed obtaining significantly higher intracellular concentrations of dapivirine as compared to the free drug ($p<0.05$), ranging from 9.4- (SLS-PCL at 2.5 µM) to 28.4-fold (SLS-PCL at 5 µM). No drug was detected when cells were incubated with 0.1 µM of free drug. Among different nanoparticle formulations, slightly but significantly higher levels were observed for SLS-PCL at 5 and 10 µM. In the case of time-dependent experiments, all nanoparticle formulations showed significantly higher drug levels than the free drug at all time points (ranging from 13.6- to 29.4-fold), peaking at around 1–2 h. From this point on, levels decreased up to 6 h but were still significantly higher than those for the free drug. Also, SLS-PCL nanoparticles presented significantly higher drug levels than the other two formulations throughout all time points.

In the case of quantitative drug uptake for DC-100 dendritic cells (Fig. 5E–F), the trend was similar to the one observed for Mo/Mac and PBMCs when comparing nanoparticles and the free drug, even if differences were smaller. For concentration-dependent experiments, the increase in intracellular drug levels was in the range of 2.6- (CTAB-PCL at 10 µM) to 14.4-fold (PEO-PCL at 1 µM), while for time-dependent experiments these values were 2.4- (CTAB-PCL at 6 h) to 7.3-fold higher (PEO-PCL at 30 min). In contrast to PBMCs, PEO-PCL nanoparticles scored significantly better than the other two formulations for both concentration- and time-dependent experiments. In the particular case of time-dependent intracellular uptake, maximum drug levels were observed after as soon as 15 min for SLS-PCL and CTAB-PCL, while moderately increasing levels were observed for PEO-PCL up to 2 h. From these points on, a reducing trend was observed for all formulations, similarly to the case of PBMCs. Lastly, SLS-PCL provided higher intracellular drug levels from 15 min to 2 h when compared to CTAB-PCL.

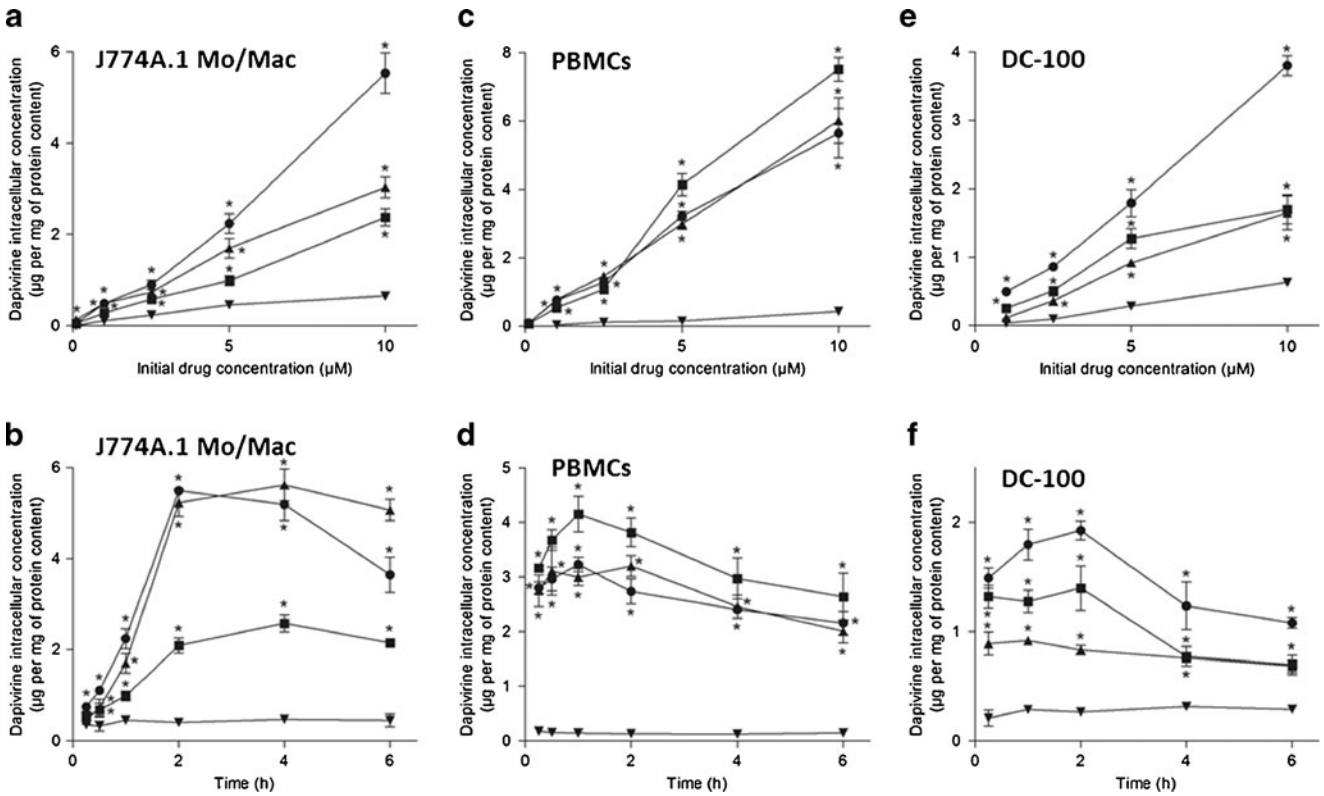


**Fig. 5** Intracellular concentration of dapivirine in J774A.1 mice monocyte/macrophages (**a**, **b**), peripheral blood mononuclear cells (PBMCs) (**c**, **d**), and DC-100 dendritic cells (**e**, **f**) as a function of initial drug concentration (**a**, **c**, **e**) and time of incubation (**b**, **d**, **f**). Incubation time was 1 h for dose-dependent studies and drug concentration was held constant at 5 $\mu$M for time-dependent studies. Concentrations are expressed as dapivirine content. Each point represents the mean value and bars the standard deviation of three independent experiments (three replicates per experiment). (*) denotes a significant difference ($p < 0.05$) when compared with the free drug. Legend: dapivirine-loaded PEO-PCL nanoparticles (●), dapivirine-loaded SLS-PCL nanoparticles (■), dapivirine-loaded CTAB-PCL nanoparticles (▲), and free dapivirine (▼).

## Antiviral Activity of Nanoparticles

The antiretroviral activity of dapivirine-loaded nanoparticles and free dapivirine as determined in the TZM-bl assay is presented in Table II. There were no significant differences in $EC_{50}$ values with mean values ranging from 1.4 to 2.4 nM. However, the toxicity to TZM-bl cells of the free drug and formulations was different resulting in changes in the selectivity index. In particular, selectivity indices for PEO-PCL and SLS-PCL nanoparticles increased more than one log when compared with the free drug, while CTAB-PCL presented a selectivity index value around 3-times lower.

In the case of the antiretroviral activity as determined in PBMCs (Table III), there were only slight differences in $EC_{50}$ when considering the continuous treatment, with values ranging from 1.5 to 3.4 nM; however, in the single treatment setting, values of $EC_{50}$ for the free drug were around 4- to 7-times higher than those for dapivirine-loaded nanoparticles. Overall, the selectivity index values for PEO-PCL and SLS-PCL formulations increased more than one log for both the single and continuous treatments when compared to those for the free drug. This increase was around 50-times in the case of single treatment. As for CTAB-PCL, the observed high antiretroviral activity was again opposed by its high toxicity, resulting in decreased selectivity index when compared to the dapivirine alone.

The antiretroviral activity of dapivirine-loaded nanoparticles and the free drug as determined in the Mo-DC/T4 cells co-culture model is presented in Table IV. Differences in $EC_{50}$ values were only slight for the continuous treatment. However, in the case of single treatment, one log higher values were observed for the free drug while this increase was lesser for nanoparticle formulations, resulting in around 7- to 13-times lower $EC_{50}$ values compared to the free drug. Also, the more favorable toxicity profile of PEO-PCL and SLS-PCL formulations allowed for relative selectivity index increases of more than one log for the single treatment. In the case of continuous treatment, this increase was more modest (10.1 and 8.2 for PEO-PCL and SLS-PCL nanoparticles, respectively). Again, CTAB-PCL presented the lowest $CC_{50}$ values which resulted in decreased selectivity index values even if in the case of single treatment the higher activity was able to yield a

**Table II** $EC_{50}$ and $CC_{50}$ Values (Mean ± Standard Deviation; $n = 3$), and Selectivity Index and Relative Selectivity Index Values (Calculated from $EC_{50}$ and $CC_{50}$ Mean Values) of Dapivirine-loaded Nanoparticles and Free Dapivirine as Determined in Luciferase Tat-Regulated Reporter Gene Assay in TZM-bl Cells

| | Free dapivirine | PEO-PCL | SLS-PCL | CTAB-PCL |
|---|---|---|---|---|
| $EC_{50}$[a] | 1.5 ± 0.2 | 2.4 ± 1.2 | 1.5 ± 0.1 | 1.4 ± 0.3 |
| $CC_{50}$[a] | 4,073 ± 1,325 | >100,000 | >100,000 | 1,161 ± 299 |
| Selectivity index | 2,715 | >41,667 | >66,667 | 829 |
| Relative selectivity index | 1 | >15.3 | >24.6 | 0.3 |

[a] Values in nM

selectivity index value 2-times higher than the one for the free dapivirine.

Lastly, nanoparticles containing no drug showed no antiviral activity up to the maximum concentration tested in all described settings, 2.3 μg/mL (corresponding to 1,000 nM of dapivirine when considering dapivirine-loaded nanoparticles).

### Cytotoxicity of Nanoparticles

Table V presents the toxicity data of nanoparticles as assessed in HEC-1-A, HeLa, VK2/E6E7, and Caco-2 cell lines. PEO-PCL nanoparticles presented $CC_{50}$ values higher than 100,000 nM for all cell lines, both in the MTS and LDH assays. SLS-PCL nanoparticles showed comparable results to free dapivirine but $CC_{50}$ values were lower in the case of VK2/E6E7 cells, contrasting with higher results for HEC-1-A, HeLa and Caco-2 cells as determined by the MTS assay. Also, the SLS-PCL formulation presented lower values for $CC_{50}$ than free dapivirine in all cell lines, as assessed by the LDH assay. $CC_{50}$ values for CTAB-PCL were consistently lower than those for free dapivirine in both the MTS and LDH assay, in some cases this reduction being of nearly one log of magnitude.

## DISCUSSION

The solvent displacement method previously optimized by Amiji *et al.* (16,17) was successfully used to produce dapivirine-loaded PCL nanoparticles with different surface properties. The obtention of PCL nanoparticles without using any surface modifier was not considered in this study since, in such conditions, uncontrolled polymer precipitation is observed (35). PCL was chosen due to its known biodegradability and favorable toxicity profile (36). Optimization of nanoparticle diameter around 200 nm was pursued because this size range seems to be optimal regarding cell uptake (37) and cervicovaginal epithelial penetration (14,15). This size range has also been shown favorable in terms of diffusion of nanoparticles through cervicovaginal fluids (38). Moreover, the simplicity of these formulations is particularly attractive for scaling-up and favorable when considering affordability issues associated with microbicide development. The release profile of dapivirine from the nanosystems is in agreement with previous studies using PCL nanoparticles (16,17), suggesting that low molecular weight molecules are rapidly released from the PLC matrix by a diffusion mechanism, whereas polymer degradation is less important to drug release. Also, the need for including a solubility enhancer in order to allow sink conditions should be taken in consideration in explaining the fast release observed. As observed by others for various polymeric dosage forms (39,40), the use of plain SFV or PBS does not yield reliable and/or quantifiable levels of drug when performing such *in vitro* studies. Indeed, drug release is expected to be different in an *in vivo* environment, where other factors (drug solubility and structure, tissue permeability, used dose) will influence the release rate. In any case, these results indicate that PCL nanoparticles may effectively release most of the incorporated dapivirine at tested pH values (4.2 and 7.4) and within a time-frame that seems appropriate for microbicide development.

In order to qualitatively characterize dapivirine intracellular delivery, we studied the ability of nanoparticles to be taken up by different cell types (VK2/E6E7, HeLa, TZM-bl, Mo/Mac, PBMCs, and dendritic cells) using fluorescence microscopy. The choice of these specific cell types is related to their genital epithelial origin or known association with HIV transmission, and hence relevant for vaginal microbicide development (8). Results showed that all formulations were able to be rapidly localized inside or, at least, associated with either epithelial or HIV-target cells. These results are in agreement with previous results obtained by Amiji *et al.* (16,17) using PEO-PCL nanoparticles, thus confirming that the use of alternative surface modifiers did not impair the ability for effective and rapid cell uptake.

Next, we proceeded with formal quantitative drug uptake studies in order to understand the dynamics of cell associated drug levels provided by nanoparticles. In the case of concentration-dependent experiments, results indicate that cell associated drug levels can be consistently increased with increasing nanoparticle concentrations, showing that, in the studied range, nanoparticle/drug

**Table III** $EC_{50}$ and $CC_{50}$ Values (Mean ± Standard Deviation; $n = 3$), and Selectivity Index and Relative Selectivity Index Values (Calculated from $EC_{50}$ and $CC_{50}$ Mean Values) of Dapivirine-Loaded Nanoparticles and Free Dapivirine as Determined in the PHA/IL-2 Stimulated PBMC Assay

| | Free dapivirine | | PEO-PCL | | SLS-PCL | | CTAB-PCL | |
|---|---|---|---|---|---|---|---|---|
| | Single[a] | Continuous[b] | Single | Continuous | Single | Continuous | Single | Continuous |
| $EC_{50}$ [c] | 49.8 ± 14.9 | 3.4 ± 2.3 | 13.1 ± 0.5 | 1.9 ± 0.3 | 7.3 ± 1.1 | 1.8 ± 0.3 | 7.9 ± 1.4 | 1.5 ± 0.2 |
| $CC_{50}$ [c] | 6,087 ± 2,478 | | ≈ 100,000 | | 39,474 ± 7,752 | | 478 ± 171 | |
| Selectivity index | 122 | 1,790 | ≈ 7,634 | ≈ 52,632 | 5,407 | 21,930 | 61 | 319 |
| Relative selectivity index | 1 | 1 | ≈ 62.6 | ≈ 29.4 | 44.3 | 12.3 | 0.5 | 0.2 |

[a] Single treatment
[b] Continuous treatment
[c] Values in nM

uptake was not saturable. Moreover, results suggest that different surface modifiers can be used for dapivirine intracellular delivery but with differential efficiency. For instance, CTAB-PCL nanoparticles provided higher intracellular concentrations of dapivirine than the two other formulations in VK2/E6E7 and HeLa cells, which can be related to the increased ability of positively charged nanoparticles to interact with the negatively charged cell membrane (41,42). This close interaction can facilitate the diffusion of the drug to the interior of the cell and/or nanoparticle uptake, mostly by chlatrin-mediated endocytosis (41), leading to increased intracellular drug concentrations. However, this was not the case for TZM-bl cells, where this type of interaction seems to be of minor importance for nanoparticle uptake and/or increasing drug diffusion into the cell. In the case of negatively charged nanoparticles, there was no or smaller differences between PEO-PCL and SLS-PCL formulations and the free drug in all three non-phagocytic cell lines (i.e. VK2/E6E7, HeLa, and TZM-bl cells). Repulsive forces due to electrostatic interaction and reduced ability of these epithelial cells to take up particles may explain these results. For instance, recent experiments by He *et al.* (43) confirm that more positive or less negative zeta potential values improve nanoparticle uptake. In general, and even if the Debye length is reduced under relatively high salt conditions such as the ones found in media, electrostatic interaction may well still be considerable upon short range distances observed at the nanoparticle/cell membrane interface level (42).

In the case of phagocytic cells (Mo/Mac, PBMCs and dendritic cells), results were noticeably different from those of epithelial cells. In all cases, there was a clear increase in the obtained intracellular drug levels when nanoparticles were used to deliver dapivirine, which can be probably explained by the extensive phagocytic uptake of nanoparticles. This indicates that developed systems provide a way for passive targeting, being particularly important due to the contribution of these cells to HIV transmission and infection (8). Variations among the different types of nanoparticles may be justified by different interaction with tested cell types and/or nanoparticle drug release dynamics. Also, results for PEO-PCL, particularly in Mo/Mac and dendritic cells, may seem contradictory as it is widely accepted that surface modification with PEO (or polyethylene glycol) is able to reduce nanoparticle uptake by phagocytic cells. However, increased drug levels can be understood in light of the relatively poor surface coverage by PEO, as indicated by the negative zeta potential of PEO-PCL nanoparticles, which allows nanoparticle formation and stabilization but does not confer enough hydrophilicity to prevent phagocytosis (44).

Maximum intracellular levels of dapivirine in phagocytic cells were achieved up to around 1–2 h for nanoparticle

**Table IV** $EC_{50}$ and $CC_{50}$ Values (Mean ± Standard Deviation; $n = 3$), and Selectivity Index and Relative Selectivity Index Values (Calculated from $EC_{50}$ and $CC_{50}$ Mean Values) of Dapivirine-Loaded Nanoparticles and Free Dapivirine as Determined in the Inhibition Assay in a Mo-DC/T4 Cells Co-culture Model

| | Free dapivirine | | PEO-PCL | | SLS-PCL | | CTAB-PCL | |
|---|---|---|---|---|---|---|---|---|
| | Single[a] | Continuous[b] | Single | Continuous | Single | Continuous | Single | Continuous |
| $EC_{50}$ [c] | 25.2 ± 6.5 | 1.8 ± 0.3 | 3.7 ± 2.5 | 1.3 ± 0.2 | 2.0 ± 0.8 | 0.8 ± 0.2 | 2.1 ± 1.0 | 0.8 ± 0.2 |
| $CC_{50}$ [c] | 10,274 ± 1,861 | | 76,984 ± 8,467 | | 38,442 ± 7,920 | | 1,728 ± 142 | |
| Selectivity index | 408 | 5,708 | 20,806 | 59,218 | 19,221 | 48,053 | 823 | 2,160 |
| Relative selectivity index | 1 | 1 | 51.0 | 10.4 | 47.1 | 8.4 | 2.0 | 0.4 |

[a] Single treatment
[b] Continuous treatment
[c] Values in nM

formulations but concentration of the drug from this time point on shows a trend to decrease. This notable observation may be explained by drug leakage from the cell after intracellular drug release from nanoparticles that were previously taken up. Two facts seem to support this statement: first, qualitative data suggests that the intracellular concentration of PCL nanoparticles is stable after peaking at 1–2 h, indicating that the particles remain inside the cell or, at least, there is a dynamic balance between endocytosis and exocytosis of nanoparticles as also described by others for vascular smooth muscle cells (45); second, the relatively fast drug release profiles observed *in vitro* for all formulations and the low molecular weight of dapivirine may favor drug leakage from inside the cell by passive diffusion. Another possibility for decreasing levels could be related to cell toxicity. However, MTS results at the highest used nanoparticle concentration and maximum incubation time tested showed no significant differences as with when compared to the control. The contribution of drug degradation to the decreasing intracellular concentrations of dapivirine is also expected to be low since *in vitro* data indicate that this drug is fairly stable in the presence of microsomal enzymes (46); moreover, in the case of the free drug, steady intracellular drug concentrations obtained after initial peaking appear to support that no important drug degradation is observed.

Another interesting fact from our quantitative results is related to the lack of correlation with the trend observed in fluorescence microscopy studies, in which the SLS-PCL nanoparticles showed consistently higher fluorescence signal, thus suggesting the possibility of being able to provide higher intracellular drug concentration. A previous study showed that SLS is able to red-shift rhodamine dyes by increasing its solubility due to the interaction of the anionic moiety of SLS and the cationic group of rhodamine dyes (47). Therefore, this mechanism may reduce dye–dye complexes formation and enhance quantum yield (48). In the case of non-ionic or cationic molecules, this interaction is not observed. Moreover, one should take in consideration that in the case of microscopy studies the variable being evaluated is nanoparticle uptake, not drug levels. Previous intracellular modeling studies by Ece Gamsiz *et al.* (18) using saquinavir-loaded PEO-PCL nanoparticles showed that the amount of drug levels is not only dependent of nanoparticle uptake but from a complex interaction between this fact, drug release from nanosystems, and the balance free drug inwards/outwards flux across the cell membrane. Thus, our studies indicate that interpretation of nanoparticle uptake results should be performed with caution and, whenever possible, complemented with actual drug levels assessment.

In order to verify if dapivirine encapsulation in nanoparticles could benefit the ability of this drug to prevent cell infection, we investigated the antiretroviral activity of the developed systems in three different cell models with

**Table V** $CC_{50}$ Values (in nM) of Dapivirine-Loaded Nanoparticles and Free Dapivirine as Determined in Different Anogenital Epithelial Cell Lines (Mean ± Standard Deviation; $n = 3$)

| | MTS | | | | LDH | | | |
|---|---|---|---|---|---|---|---|---|
| | HEC-1-A | HeLa | VK2/E6E7 | Caco-2 | HEC-1-A | HeLa | VK2/E6E7 | Caco-2 |
| PEO-PCL | > 100,000 | > 100,000 | > 100,000 | > 100,000 | > 100,000 | > 100,000 | > 100,000 | > 100,000 |
| SLS-PCL | > 100,000 | > 100,000 | 18,469 ± 2,426 | > 100,000 | 59,702 ± 8,867 | 52,692 ± 8,663 | 47,979 ± 4,391 | 57,613 ± 6,298 |
| CTAB-PCL | 6,851 ± 2,690 | 17,330 ± 2334 | 10,999 ± 2,048 | 2,672 ± 505 | 40,787 ± 3,512 | 15,037 ± 4,207 | 14,444 ± 2,721 | 13,930 ± 3,422 |
| Free dapivirine | 17,026 ± 1,868 | 26,642 ± 4,434 | 64,822 ± 9,802 | 11,760 ± 1,569 | > 100,000 | > 100,000 | 77,487 ± 6513 | 73,891 ± 6,777 |

increasing relevance for microbicide development. In particular, the Mo-DC/T4 co-culture model is considered a more physiologically relevant setting for microbicides as it represents the primary target cells and their cross-talk upon sexual HIV transmission (23). Also, the potential therapeutic usefulness of nanoparticles was assessed by calculating the selectivity index values in these models. Overall, the results of antiretroviral assays confirmed the high potency of dapivirine, presenting $EC_{50}$ values in the nanomolar range in accordance with previously published results (25,28,49). The encapsulation of dapivirine in different nanoparticles did not reduce the antiretroviral activity of the drug. In fact, results obtained from both the PBMC and Mo-DC/T4 co-culture models suggest that these systems may be advantageous, particularly when considering the data obtained with the single treatment setting. Indeed, the higher level of protection conferred by dapivirine-loaded nanoparticles might be closely related to the ability of nanoparticle formulations to increase and sustain cell association of dapivirine with PBMCs and dendritic cells but not TZM-bl cells, as shown in the uptake studies. In fact, the phagocytic nature of the cells used in the PBMCs and Mo-DC/T4 models, contrasting with the non-phagocytic ability of TZM-bl cells (derived from the HeLa cervical cell line), reinforces the importance of the results previously observed in the quantitative uptake studies. However, this effect also seems to fade away with continuous use which we hypothesize may be related to the complete drug release from nanoparticles after several hours. As evidenced in the quantitative evaluation of intracellular drug levels, particularly in phagocytic cells, after peaking around 1–2 h, dapivirine levels drop with time and eventually reach basal levels as for the free drug. Additionally, the obtained cytotoxicity data in the tested settings gives way to additional advantage of PEO-PCL and SLS-PCL nanoparticles as substantially higher selectivity indices can be achieved. In the case of the CTAB-PCL formulation, high cellular toxicity seems to limit its possible use.

Finally, we investigated the *in vitro* toxicity of nanoparticles in epithelial cells from female genital and anorectal origin. Cytotoxicity results for free dapivirine are in close agreement with those recently published (29,34). The *in vitro* toxicity profile of dapivirine showed to be improved for the PEO-PCL formulation and comparable to the free drug in the case of the SLS-PCL formulation. However, the moderately increased cytotoxicity of SLS-PCL as assessed by the LDH assay should be taken into consideration. These results are not surprising considering that SLS is an anionic detergent and, therefore, able to interact with the cell membrane and increase its leakiness. Still, the low concentrations of SLS used, as required for the formulation of SLS-PCL nanoparticles, are much smaller than those reported to induce cytotoxicity

(29). The results for CTAB-PCL nanoparticles confirm those obtained by the WST-1 for calculating the selectivity index and compromise the possible use of this formulation in the future. This may be justified not only by the inherent toxicity of CTAB, as it is known that cationic surfactants usually show high cytoxicity, but also by the generally higher toxicity of positively-charged nanoparticles. In the case of PEO-PCL nanoparticles, the improved cytotoxicity profile seems to be associated with the recognized safety of its components and, possibly, to the ability to reduce the concentration of dapivirine to which the cells are in fact exposed. Indeed, and even if the *in vitro* drug release results presented above indicate that nearly all dapivirine is rapidly released in media containing a solubilizing agent (i.e. polysorbate 80), the absence of sink conditions in cell culture conditions may yield sustained drug release from nanoparticles. Although the total amount of drug inside cells is increased, namely in phagocytic cells, our studies are not able to distinguish between the fraction of free-drug and nanoparticle associated drug. Finally, the results obtained for Caco-2, a colorectal epithelial cell line, provide some evidence that the PEO-PCL and SLS-PCL formulations may also be useful for the development of a rectal microbicide.

Even if the overall results provide substantial insights on the potential and drawbacks of differently engineered dapivirine-loaded PCL nanoparticles in the development of microbicides, other questions will require further investigation. For instance, these nanosized systems need to be formulated in an adequate pharmaceutical dosage form in order to allow vaginal (or rectal) administration, spreading and retention. Because of their versatility, gels will most likely be a valid option (50). Another question is related to the interaction of developed nanoparticles with cervicovaginal fluids and mucosa. Important information can be inferred from previous studies (14,15,38,51), but specific testing for the developed PCL nanoparticles are in order. Data from our group indicates that these nanoparticles are able to migrate, mostly by sub-diffusive transport, through a mucin network that resembles the natural fluid present in the human vagina (52), which is deemed essential in order to achieve the mucosal tissue (53). In the present work, the study of the antiviral activity was limited to the use of one relevant virus strain model for the development of microbicides; however, the validity of the present results could also be expanded by testing other viruses, including CXCR4-tropic viruses.

## CONCLUSION

Dapivirine is one of the most promising drug candidates in the microbicides pipeline. Although presenting high activity against HIV-1, this molecule requires adequate formulation in order to potentiate its antiretroviral properties while reducing its toxicity. Even if currently available clinical trials found it safe for use as a vaginal microbicide (54,55), dapivirine would still benefit from strategies that allow increasing its selectivity/therapeutic indices. Data discussed in this study seem to indicate that the incorporation of dapivirine in differently surface engineered PCL nanoparticles can influence drug levels associated with particular cell types. For instances, passive targeting to HIV-target cells was observed, possibly due to their phagocytic nature. This is in contrast with the results obtained for nanoparticles and free dapivirine when tested in cells of epithelial origin. Also, increased antiviral activity and reduced/comparable cytoxicity could be achieved in the case of PEO-PCL and SLS-PCL nanoparticles. We hypothesize that these results, particularly when short-course treatment is considered, are intimately related to the ability of nanoparticles to increase the intracellular drug levels in HIV target cells, while allowing the drug to be released in a sustained fashion, thus making it possible to limit its cytoxicity. Also, toxicity profiles in female genital and anorectal cell lines showed to be favorable or not, according to specific nanoparticle surface properties. These results provide evidence for the value of nanotechnology-based approaches towards the development of improved vaginal and rectal microbicides. In particular, dapivirine-loaded PEO-PCL nanoparticles deserve further investigation.

## ACKNOWLEDGMENTS & DISCLOSURES

José das Neves gratefully acknowledges Fundação para a Ciência e a Tecnologia, Portugal for financial support (grant SFRH/BD/43393/2008). Kevin K. Ariën and Guido Vanham are supported by research grants from the Fund for Scientific Research Flanders (FWO), the Agence Nationale de Recherches sur le SIDA et les hépatites virales (ANRS), and EU-FP7 CHAARM. Dapivirine was originally developed by Tibotec Pharmaceuticals and was licensed to the International Partnership for Microbicides under a royalty-free agreement for the development of vaginal microbicides. We express our gratitude to Jing Xu for SEM imaging at the Nanomaterials Characterization Facility, Northeastern University.

## REFERENCES

1. Cohen MS, Hellmann N, Levy JA, DeCock K, Lange J. The spread, treatment, and prevention of HIV-1: evolution of a global pandemic. J Clin Invest. 2008;118(4):1244–54.
2. Grant RM, Lama JR, Anderson PL, McMahan V, Liu AY, Vargas L, *et al.* Preexposure chemoprophylaxis for HIV prevention in men who have sex with men. N Engl J Med. 2010;363(27):2587–99.

3. Morris GC, Lacey CJ. Microbicides and HIV prevention: lessons from the past, looking to the future. Curr Opin Infect Dis. 2010;23(1):57–63.
4. Abdool Karim Q, Abdool Karim SS, Frohlich JA, Grobler AC, Baxter C, Mansoor LE, *et al.* Effectiveness and safety of tenofovir gel, an antiretroviral microbicide, for the prevention of HIV infection in women. Science. 2010;329(5996):1168–74.
5. Ariën KK, Vanham G. First real success for anti-HIV gel: a new start for HIV microbicides? Future Microbiol. 2010;5:1621–3.
6. Hladik F, McElrath MJ. Setting the stage: host invasion by HIV. Nat Rev Immunol. 2008;8(6):447–57.
7. Shen R, Richter HE, Clements RH, Novak L, Huff K, Bimczok D, *et al.* Macrophages in vaginal but not intestinal mucosa are monocyte-like and permissive to human immunodeficiency virus type 1 infection. J Virol. 2009;83(7):3258–67.
8. Ariën KK, Jespers V, Vanham G. HIV sexual transmission and microbicides. Rev Med Virol. 2011;21(2):110–33.
9. Kashuba AD, Abdool Karim SS, Kraft E, White N, Sibeko S, Werner L, *et al.* Do systemic and genital tract tenofovir concentrations predict HIV seroconversion in the CAPRISA 004 tenofovir gel trial? XVIII International AIDS Conference, 2010, Vienna, Austria.
10. Rohan LC, Sassi AB. Vaginal drug delivery systems for HIV prevention. AAPS J. 2009;11(1):78–87.
11. du Toit LC, Pillay V, Choonara YE. Nano-microbicides: challenges in drug delivery, patient ethics and intellectual property in the war against HIV/AIDS. Adv Drug Deliv Rev. 2010;62(4–5):532–46.
12. das Neves J, Amiji MM, Bahia MF, Sarmento B. Nanotechnology-based systems for the treatment and prevention of HIV/AIDS. Adv Drug Deliv Rev. 2010;62(4–5):458–77.
13. Mallipeddi R, Rohan LC. Nanoparticle-based vaginal drug delivery systems for HIV prevention. Expert Opin Drug Deliv. 2010;7(1):37–48.
14. Ham AS, Cost MR, Sassi AB, Dezzutti CS, Rohan LC. Targeted delivery of PSC-RANTES for HIV-1 prevention using biodegradable nanoparticles. Pharm Res. 2009;26(3):502–11.
15. Woodrow KA, Cu Y, Booth CJ, Saucier-Sawyer JK, Wood MJ, Saltzman WM. Intravaginal gene silencing using biodegradable polymer nanoparticles densely loaded with small-interfering RNA. Nat Mater. 2009;8(6):526–33.
16. Chawla JS, Amiji MM. Biodegradable poly(epsilon-caprolactone) nanoparticles for tumor-targeted delivery of tamoxifen. Int J Pharm. 2002;249(1–2):127–38.
17. Shah LK, Amiji MM. Intracellular delivery of saquinavir in biodegradable polymeric nanoparticles for HIV/AIDS. Pharm Res. 2006;23(11):2638–45.
18. Ece Gamsiz D, Shah LK, Devalapally H, Amiji MM, Carrier RL. A model predicting delivery of saquinavir in nanoparticles to human monocyte/macrophage (Mo/Mac) cells. Biotechnol Bioeng. 2008;101(5):1072–82.
19. das Neves J, Sarmento B, Amiji MM, Bahia MF. Development and validation of a rapid reversed-phase HPLC method for the determination of the non-nucleoside reverse transcriptase inhibitor dapivirine from polymeric nanoparticles. J Pharm Biomed Anal. 2010;52(2):167–72.
20. Owen DH, Katz DF. A vaginal fluid simulant. Contraception. 1999;59(2):91–5.
21. Frenkel YV, Clark Jr AD, Das K, Wang YH, Lewi PJ, Janssen PA, *et al.* Concentration and pH dependent aggregation of hydrophobic drug molecules and relevance to oral bioavailability. J Med Chem. 2005;48(6):1974–83.
22. Cavrois M, Neidleman J, Kreisberg JF, Greene WC. *In vitro* derived dendritic cells trans-infect CD4 T cells primarily with surface-bound HIV-1 virions. PLoS Pathog. 2007;3(1):e4.
23. Vanham G, Penne L, Allemeersch H, Kestens L, Willems B, van der Groen G, *et al.* Modeling HIV transfer between dendritic cells and T cells: importance of HIV phenotype, dendritic cell-T cell contact and T-cell activation. AIDS. 2000;14(15):2299–311.
24. Van Herrewege Y, Penne L, Vereecken C, Fransen K, van der Groen G, Kestens L, *et al.* Activity of reverse transcriptase inhibitors in monocyte-derived dendritic cells: a possible *in vitro* model for postexposure prophylaxis of sexual HIV transmission. AIDS Res Hum Retroviruses. 2002;18(15):1091–102.
25. Van Herrewege Y, Vanham G, Michiels J, Fransen K, Kestens L, Andries K, *et al.* A series of diaryltriazines and diarylpyrimidines are highly potent nonnucleoside reverse transcriptase inhibitors with possible applications as microbicides. Antimicrob Agents Chemother. 2004;48(10):3684–9.
26. Sallusto F, Lanzavecchia A. Efficient presentation of soluble antigen by cultured human dendritic cells is maintained by granulocyte/macrophage colony-stimulating factor plus interleukin 4 and downregulated by tumor necrosis factor alpha. J Exp Med. 1994;179(4):1109–18.
27. Freshney RI. Culture of animal cells: a manual of basic technique and specialized applications. 6th ed. Hoboken: Wiley-Blackwell; 2010. p. 365–82.
28. Van Herrewege Y, Michiels J, Van Roey J, Fransen K, Kestens L, Balzarini J, *et al. In vitro* evaluation of nonnucleoside reverse transcriptase inhibitors UC-781 and TMC120-R147681 as human immunodeficiency virus microbicides. Antimicrob Agents Chemother. 2004;48(1):337–9.
29. Gali Y, Delezay O, Brouwers J, Addad N, Augustijns P, Bourlet T, *et al. In vitro* evaluation of viability, integrity and inflammation in genital epithelia upon exposure to pharmaceutical excipients and candidate microbicides. Antimicrob Agents Chemother. 2010;54(12):5105–14.
30. Kanemura Y, Mori H, Kobayashi S, Islam O, Kodama E, Yamamoto A, *et al.* Evaluation of *in vitro* proliferative activity of human fetal neural stem/progenitor cells using indirect measurements of viable cells based on cellular metabolic activity. J Neurosci Res. 2002;69(6):869–79.
31. Montefiori DC. Evaluating neutralizing antibodies against HIV, SIV, and SHIV in luciferase reporter gene assays. Curr Protoc Immunol. 2005;Chapter 12:Unit 12.11.
32. Montefiori DC. Measuring HIV neutralization in a luciferase reporter gene assay. Methods Mol Biol. 2009;485:395–405.
33. Heyndrickx L, Vermoesen T, Vereecken K, Kurth J, Coppens S, Aerts L, *et al.* Antiviral compounds show enhanced activity in HIV-1 single cycle pseudovirus assays as compared to classical PBMC assays. J Virol Methods. 2008;148(1–2):166–73.
34. Gali Y, Ariën KK, Praet M, Van den Bergh R, Temmerman M, Delezay O, *et al.* Development of an *in vitro* dual-chamber model of the female genital tract as a screening tool for epithelial toxicity. J Virol Methods. 2010;165(2):186–97.
35. Sinha VR, Bansal K, Kaushik R, Kumria R, Trehan A. Poly-epsilon-caprolactone microspheres and nanospheres: an overview. Int J Pharm. 2004;278(1):1–23.
36. Woodruff MA, Hutmacher DW. The return of a forgotten polymer—polycaprolactone in the 21st century. Prog Polym Sci. 2010;35(10):1217–56.
37. Conner SD, Schmid SL. Regulated portals of entry into the cell. Nature. 2003;422(6927):37–44.
38. Lai SK, O'Hanlon DE, Harrold S, Man ST, Wang YY, Cone R, *et al.* Rapid transport of large polymeric nanoparticles in fresh undiluted human mucus. Proc Natl Acad Sci U S A. 2007;104(5):1482–7.
39. Woolfson AD, Malcolm RK, Morrow RJ, Toner CF, McCullagh SD. Intravaginal ring delivery of the reverse transcriptase inhibitor TMC 120 as an HIV microbicide. Int J Pharm. 2006;325(1–2):82–9.
40. Gupta KM, Pearce SM, Poursaid AE, Aliyar HA, Tresco PA, Mitchnik MA, *et al.* Polyurethane intravaginal ring for controlled delivery of dapivirine, a nonnucleoside reverse transcriptase inhibitor of HIV-1. J Pharm Sci. 2008;97(10):4228–39.

41. Harush-Frenkel O, Rozentur E, Benita S, Altschuler Y. Surface charge of nanoparticles determines their endocytic and transcytotic pathway in polarized MDCK cells. Biomacromolecules. 2008;9(2):435–43.
42. Harush-Frenkel O, Altschuler Y, Benita S. Nanoparticle–cell interactions: drug delivery implications. Crit Rev Ther Drug Carrier Syst. 2008;25(6):485–544.
43. He C, Hu Y, Yin L, Tang C, Yin C. Effects of particle size and surface charge on cellular uptake and biodistribution of polymeric nanoparticles. Biomaterials. 2010;31(13):3657–66.
44. Bazile D, Prud'homme C, Bassoullet MT, Marlard M, Spenlehauer G, Veillard M. Stealth Me.PEG-PLA nanoparticles avoid uptake by the mononuclear phagocytes system. J Pharm Sci. 1995;84(4):493–8.
45. Panyam J, Labhasetwar V. Dynamics of endocytosis and exocytosis of poly(D, L-lactide-co-glycolide) nanoparticles in vascular smooth muscle cells. Pharm Res. 2003;20(2):212–20.
46. Lewi P, Arnold E, Andries K, Bohets H, Borghys H, Clark A, *et al.* Correlations between factors determining the pharmacokinetics and antiviral activity of HIV-1 non-nucleoside reverse transcriptase inhibitors of the diaryltriazine and diarylpyrimidine classes of compounds. Drugs R D. 2004;5(5):245–57.
47. Tajalli H, Ghanadzadeh Gilani A, Zakerhamidi MS, Moghadam M. Effects of surfactants on the molecular aggregation of rhodamine dyes in aqueous solutions. Spectrochim Acta A Mol Biomol Spectrosc. 2009;72(4):697–702.
48. Arbeloa FL, Ojeda PR, Arbeloa IL. Dimerization and trimerization of rhodamine 6G in aqueous solution. Effect on the fluorescence quantum yield. J Chem Soc [Perkin 1]. 1988;84 (12):1903–12.
49. Terrazas-Aranda K, Van Herrewege Y, Lewi PJ, Van Roey J, Vanham G. *In vitro* pre- and post-exposure prophylaxis using HIV inhibitors as microbicides against cell-free or cell-associated HIV-1 infection. Antivir Chem Chemother. 2007;18(3):141–51.
50. das Neves J, Bahia MF. Gels as vaginal drug delivery systems. Int J Pharm. 2006;318(1–2):1–14.
51. das Neves J, Amiji M, Sarmento B. Mucoadhesive nanosystems for vaginal microbicide development: friend or foe? Wiley Interdiscip Rev Nanomed Nanobiotechnol. 2011;3(4):389–99.
52. das Neves J, Sarmento B, Bahia MF, Carrier RL, Amiji M. Development and characterization of dapivirine-loaded poly (ε-caprolactone) nanoparticles as novel vaginal microbicide drug delivery systems. Trends in Microbicide Formulation Workshop, 2010, Arlington, VA, USA.
53. das Neves J, Bahia MF, Amiji MM, Sarmento B. Mucoadhesive nanomedicines: characterization and modulation of mucoadhesion at the nanoscale. Expert Opin Drug Deliv. 2011;8(8):1085–104.
54. Nel A, Smythe S, Young K, Malcolm K, McCoy C, Rosenberg Z, *et al.* Safety and pharmacokinetics of dapivirine delivery from matrix and reservoir intravaginal rings to HIV-negative women. J Acquir Immune Defic Syndr. 2009;51(4):416–23.
55. Nel AM, Coplan P, van de Wijgert JH, Kapiga SH, von Mollendorf C, Geubbels E, *et al.* Safety, tolerability, and systemic absorption of dapivirine vaginal microbicide gel in healthy, HIV-negative women. AIDS. 2009;23(12):1531–8.